Clean Energy Technologies Journal
Web page info: https://cetj.yildiz.edu.tr
DOI: 10.14744/cetj.2025.0004

CLEAN ENERGY TECHNOLOGIES JOURNAL

Research Article

Post-disaster EV dispatch for powering base stations: A MILP approach to maximize spatiotemporal coverage

Ramazan KILIÇ[1*], Alper Kağan CANDAN[2], Ali Rıfat BOYNUEĞRİ[3]

[1]*Department of Energy Technologies, Yildiz Technical University, Istanbul, Türkiye*
[2]*Department of Electrical and Electronics Engineering, Manisa Celal Bayar University, Manisa, Türkiye*
[3]*Department of Electrical Engineering, Yildiz Technical University, Istanbul, Türkiye*

ARTICLE INFO

Article history
Received: 11 December 2025
Revised: 25 December 2025
Accepted: 02 January 2026

Key words:
Emergency Energy Management; EV Fleet Management; MILP; Population-Based Temporal Coverage; Post-Disaster Communication; Resilience.

ABSTRACT

Disasters frequently disable the electrical grid, jeopardizing communication infrastructure and causing severe disruptions in emergency communications. Ensuring rapid deployment of power sources for base stations (BSs) is therefore critical in post-disaster conditions. This study presents a mixed-integer linear programming (MILP) framework that dispatches a fleet of electric vehicles (EVs) to energize multiple BSs and maximizes population-based temporal communication coverage (people × time). In a case study involving 20 BSs and 10 EVs, the optimization prioritizes early service to densely populated areas and delivers a total of 17,597 people for 228 minutes of communication access. Although the served population gradually declines as the energy of the EV fleet depletes, the connectivity is sustained until 16:34. Results demonstrate that feasible EV–BS assignments and service durations are obtained considering BS power demand, coverage areas, and EV initial energy parameters. The proposed model enables communication availability after disasters without relying on additional fixed power resources.

Cite this article as: Kılıç R, Candan AK, Boynueğri AR. Post-disaster EV dispatch for powering base stations: a MILP approach to maximize spatiotemporal coverage. Clean Energy Technol J 2025;3(2):39–49.

INTRODUCTION

In recent years, natural hazards, particularly earthquakes and floods, have increasingly threatened critical infrastructure systems. Power outages following such events trigger cascading service disruptions, severely interrupting daily life. Among the most rapidly affected are communication networks, whose continuity is indispensable during post-disaster response and recovery [1]. The earthquake centered in Kahramanmaraş, Türkiye, starkly revealed this vulnerability: of the 8,900 cellular base stations (BSs) across the ten affected provinces, 2,451 (28%) became non-operational. Although more than 400 mobile BSs with satellite backhaul were deployed, their operation relied on diesel generators (DGs) capable of providing only 3–4 hours of autonomy. Repeated service interruptions occurred due to severe fuel-logistics constraints [2,3]. Ensuring a stable power supply for BSs, the backbone of cellular communi-

*Corresponding author
*E-mail adress: ramazan.kilic@std.yildiz.edu.tr

cation networks, therefore becomes a major challenge under disaster conditions. Traditional power sources are often inaccessible or insufficient, highlighting the need for flexible and rapidly deployable alternatives. Previous research has explored hybrid architectures. Rahman et al. [4] proposed a resilient hybrid energy system (RHES) integrating photovoltaic (PV) generation, proton exchange membrane (PEM) fuel cells, and battery energy storage coordinated through an intelligent energy management system (EMS). The RHES was designed to autonomously supply Base Transceiver Stations (BTS) in grid-independent emergency scenarios. Simulation results demonstrated that BTS operability could be sustained even during prolonged outages, thereby maintaining reliable communication services. Similarly, Ünal and Dağteke [1] developed PV fuel cell hybrid systems capable of providing uninterrupted renewable power to BS following disasters. In addition, Okundamiya et al. conducted a comprehensive assessment of renewable-energy-based hybrid power systems for mobile telecommunication sites, demonstrating that PV–wind–battery configurations can significantly reduce operational costs and enhance BS power reliability in regions with unstable grid access[5]. In a comprehensive survey, Cabrera-Tobar et al. emphasized the vulnerability of telecommunication infrastructure, particularly BSs, to power interruptions stemming both from technical failures and climate-induced hazards. To mitigate these risks, the authors examined a broad set of resilience strategies structured around the phases of preparedness, response, and recovery, including mobile DGs, electric vehicle (EVs) fleets, energy storage systems (ESSs), and stand-alone microgrids (MGs) [6]. Rudenko et al. [7] similarly highlighted that replacing DGs used for mobile BSs with hybrid systems combining hydrogen fuel cells, solar power, and wind energy can ensure reliable off-grid operation while reducing environmental impacts. Such hybrid configurations play a key role in enhancing the sustainability and resilience of telecommunication systems.

Motivated by the growing need for rapidly deployable power solutions for communication systems in post-disaster conditions, this study proposes an optimization-based framework for supplying energy to BS using EVs. The model jointly determines the allocation and scheduling of multiple EVs, each with a distinct initial state of energy (SOE), to BS that differ in power requirements and coverage areas [8]. The objective is to identify the most effective EV–BS matching by maximizing a population–temporal accessibility metric, defined as the product of the number of communications served people and the duration of service provision. The primary contributions of this work are summarized as follows.

A post-disaster EV fleet management framework designed to sustain and extend the operational availability of cellular communication services by supplying emergency power to BS.

Highlights

- MILP model optimizes EV dispatch and BS activation under energy limits
- Cell-based population metrics maximize spatiotemporal coverage.
- Framework extends BS operation without fixed power infrastructure.

A rigorous optimization model that, under EV energy and mobility constraints, determines optimal EV–BS allocation strategies to maximize population-temporal accessibility during disaster-induced grid outages.

The remainder of this article is organized as follows. Section 2 (*Methodology*) describes the overall system model, outlines the modeling assumptions, and formally states the problem. This section also elaborates on the population–time accessibility metric, together with the decision variables and the full set of optimization constraints. Section 3 (*Results*) presents the case study configuration, parameterization, and numerical results derived from the proposed framework. Finally, Section 4 (*Conclusions*) provides a comprehensive synthesis of the findings, interprets the implications of the results for post-disaster communication resilience, and highlights promising avenues for future research.

MATERIALS AND METHODS

This study examines a post-disaster scenario in which cellular BS are subjected to a prolonged grid outage and an EV fleet is deployed as a mobile power supply resource. Each BS is characterized by a fixed power demand and an associated population density within its coverage area, while each EV is defined by its initial SOE and maximum power delivery capability. Since the number of BSs exceeds the number of available EVs, only a limited subset of BSs can be energized at any given time. Moreover, heterogeneous BS types possess different coverage capabilities and consequently differ in the number of users they can serve. Under these conditions, the system operator must determine, over a finite planning horizon, which BS will be energized by each EV while considering the activation duration of each EV–BS assignment. To address this decision-making problem, an EV dispatch strategy is formulated as a mixed-integer linear programming (MILP) optimization model.

EV–BS Spatial Configuration and Distance Computation

The primary objective of the proposed optimization algorithm is to maximize the cumulative population–time accessibility (people × time) by ensuring the continuous energization of BS throughout the disruption horizon following a disaster. Let the discrete time domain be represented by

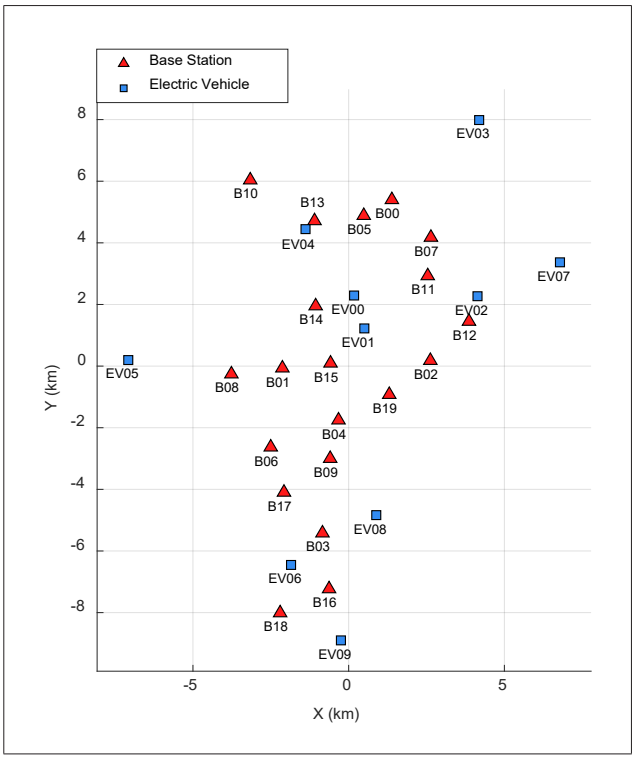

Figure 1. Cartesian coordinates of EV and BS.

$t \in T$, the set of BSs by $b \in B$, and the set of EVs, utilized as mobile power sources, by $e \in E$. Prior to the disaster event, the spatial positions of the EV fleet are defined in a Cartesian coordinate system as $X_e^{EV} \in \mathbb{R}^2$ (1), while the geographical locations of the BS are similarly represented as $X_b^{BS} \in \mathbb{R}^2$ (2), as illustrated in Figure 1. Based on these spatial representations, the Euclidean distance between each EV and each BS at the initial time step $t = 0$ is denoted by $\beta_{e,b}$ (3). Using this rate, the total travel energy required for EV e to reach BS b is computed as $E_{e,b}^{\text{travel}}$ (4). These definitions collectively establish the fundamental spatial and energetic relationships governing the EV–BS assignments within the proposed optimization framework.

$$X_e^{EV} = (x_e^{EV}, y_e^{EV}) \in R^2 \quad (1)$$

$$X_b^{BS} = (x_b^{BS}, y_b^{BS}) \in R^2 \quad (2)$$

$$\beta_{[e,b]} = \sqrt[2]{(x_e^{EV} - x_b^{BS})^2 + (y_e^{EV} - y_b^{BS})^2 [km]} \quad (3)$$

$$E_{e,b}^{travel} = \gamma . \beta_{[e,b]} \ [watt.min] \quad (4)$$

Once an EV arrives at its determined BS, it immediately initiates the power supply. The corresponding travel time required for EV e to reach BS b is formally denoted as $t_{\text{arr}(e,b)}$ (5).

$$t_{arr[e,b]} = \left\lceil \frac{\beta_{[e,b]}}{V_{ev}} \right\rceil [min] \quad (5)$$

$$\Delta_{[t,e,b]} = 1 \begin{cases} 1, & t = t_{arr[e,b]} \\ 0, & otherwise \end{cases} \quad (6)$$

The variable $\Delta_{t,e,b}$ (6) is defined as a binary indicator specifying whether EV e has arrived at BS b at time t. The indicator takes the value $\Delta_{t,e,b} = 1$ when the EV reaches the corresponding BS, and $\Delta_{t,e,b} = 0$ otherwise. For each EV–BS pair, the arrival event can occur at most once; therefore, $\Delta_{t,e,b} = 1$ may be assigned at exactly one time step for every (e, b) pair (7).

$$\sum_{t=1}^{AS-1} \Delta_{[t,e,b]} = 1 \quad (7)$$

Coverage Cells and Population Density

The computation of cumulative population–time communication access and population density in this study is carried out over a cell-based grid system. The two-dimensional grid is constructed using a uniform coordinate structure defined along the X and Y axes, with each grid cell represented by its centroid, denoted as $X_i = (x_i, y_i)$. The grid dimensions are given by $\lfloor X \rfloor \times \lfloor Y \rfloor$, and the total number of cells is denoted by C. Each grid cell has a side length of D [km], and its area is defined as $A_{\text{cell}} = PCA = D^2$[km²].

For each BS $b \in B = \{1, \ldots, B\}$, a coordinate vector X_b^{BS}(2) and a coverage radius r_b are defined. Using these parameters, a coverage matrix $S_{b,c} \in \{0,1\}^{B \times C}$ is constructed for all grid cells. The matrix entry $S_{b,c} = 1$ if cell c lies within the coverage area of BS b, and $S_{b,c} = 0$ otherwise. In addition, a binary variable $N_{b,c}$ (8) is introduced to indicate whether cell c is covered by at least one BS.

$$N_{b,c} = 1\left\{\sum_{b \in B} S_{b,c} > 0\right\} \quad (8)$$

To spatially represent post-disaster population density within the model, macro-circles (macro coverage areas) are defined. For each macro-circle $m \in M$, the center coordinates $c_m = (x_m, y_m)$, the radius R_m, the central population density $\rho_m^{(\text{center})}$, and the edge population density $\rho_m^{(\text{edge})}$ are specified. The Euclidean distance between the center of macro-circle m and the center of grid cell c is computed by $d_m(i)$, as given in Equation (9).

$$d_m(i) = \sqrt{\sum_{j=1}^{p} (x_{i,j} - c_{m,j})^2} \quad (9)$$

If the $d_m(i) \leq R_m$, the cell is considered within the coverage area of macro-circle m. In this case, the population density assigned to the cell is computed as $\rho_m(i)$ (10) Inside the macro-circle $d_m(i) \leq R_m$.

$$\rho_m(i) = \rho_m^{edge} + \left(\rho_m^{center} - \rho_m^{edge}\right) \left(1 - \frac{d_m(i)}{R_m}\right) \quad (10)$$

Not contained within macro-circle m, where $d_m(i) > R_m$:

$$\rho_m(i) = 0 \quad (11)$$

A linear decay function is defined for the macro-circle population density such that the density attains its maximum value at the macro-circle center and decreases to a minimum at the outermost cells. If a cell lies beyond the macro-circle, its population density is assigned as $\rho_m(i) = 0$ (11). Since a cell may fall within the coverage areas of multiple macro-circles, the final macro-circle population density is determined as $\rho_{max}(i)$ (12) which corresponds to the maximum value among all macro-circles for that cell.

$$\rho_{max}(i) = {}^{max}_{m}\rho_m(i) \quad (12)$$

Finally, the overall population density for each cell is defined as ρ_c. If the cell lies within macro-circles, its value is assigned as $\rho_c = \rho_{\max}(i)$. For cells outside the macro-circles, the density is determined based on their coverage status, ensuring a seamless transition between high-density macro regions and the surrounding settlement area. In this manner, a continuous, cell-based population density function is established across the entire study region.

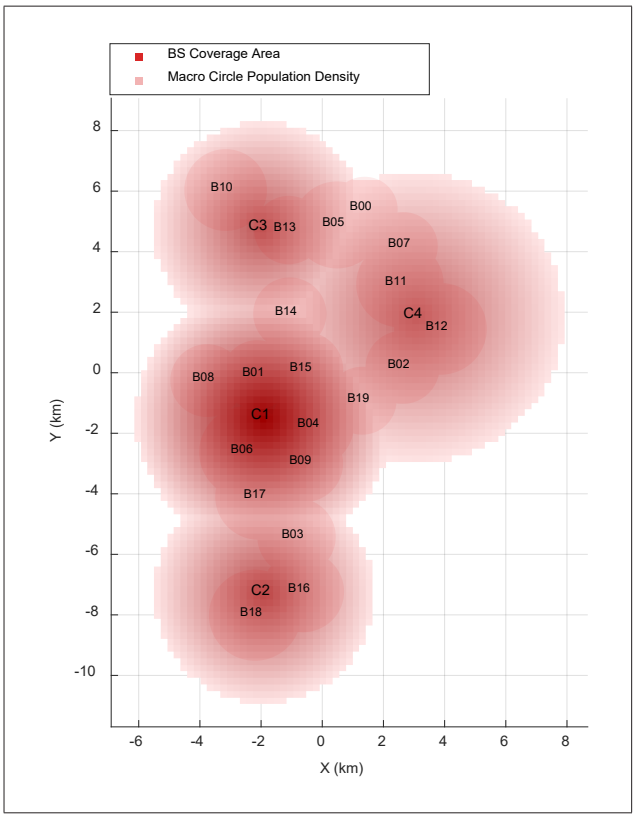

Figure 2. Coverage areas of the BSs and the population density distribution.

Through this formulation, the population density can be represented on the grid plane as a parametric and computationally tractable function, allowing coverage maps to be directly integrated into the optimization model. In post-disaster scenarios in particular, these macro regions correspond to critical settlement areas. Figure 2. presents the resulting population density map, which includes both the macro regions and the coverage areas of the BSs.

Energy and EV–Base Station Matching

The total amount of energy that can be supplied to all BSs is constrained by the initial SOE of the EV fleet (13).

$$PS_{max} = \sum_{e=1}^{E} SOE_e^{\text{init}} \, [Watt.min] \quad (13)$$

At the beginning of the disaster response, each EV is required to be assigned to a single BS. To represent this allocation, the binary variable $B_{e,b}^{EV,L}$ is introduced, indicating whether

EV e is assigned to BS b. This formulation ensures that every EV is allocated to only one BS.

$$\sum_{b=1}^{B} B_{e,b}^{EV,L} = 1 \quad (14)$$

In addition, to ensure that each BS can receive at most one EV:

$$\sum_{e=1}^{E} B_{e,b}^{EV,L} \leq 1 \quad (15)$$

The EV–BS assignment is modeled as a one-to-one matching. This structure prevents any vehicle from being assigned to multiple BSs simultaneously and likewise ensures that no more than one vehicle is located at a given BS. As a result, the distribution of energy across BSs becomes balanced and operationally manageable.

This equality expresses, in a time-traceable manner, the BS to which each EV is assigned. For this purpose, a continuous index variable $EV_{t,e}$ (16) is defined. The BS assignment determined for each EV at the beginning of the disaster remains fixed throughout the entire time horizon; this requirement is enforced by the following equality:

$$EV_{[t,e]} = \sum_{b=0}^{TBSN-1} b.B_{e,b}^{EV,L} \quad (16)$$

Base Station Energy Balance

The time-dependent SOE for each BS is denoted by $\text{SOE}_{(t,b)}^{BS}$ (19). This SOE level is updated through an energy-balance equation that incorporates the previous SOE $\text{SOE}_{(t-1,b)}^{BS}$, the energy

consumed during the preceding time step $P_{(t-1,b)}^{(BS,A)}$, and the net amount of energy delivered by an EV upon arrival $\mathrm{SOE}_{(t,b)}^{arr}$ (17). In this statement, SOE_{e}^{init} denotes the initial energy available in EV e, while $E_{(e,b)}^{travel}$ represents the amount of energy the vehicle must expend to reach BS b. Prior to the beginning of the disaster, the initial SOE of all BSs is assumed to be zero, i.e., $\mathrm{SOE}_{(0,b)}^{BS} = 0$ (18).

$$SOE_{t,b}^{arr} = \sum_{e=0}^{TEVN-1} B_{e,b}^{EV,L}.(SOE_{e}^{init} - E_{e,b}^{travel}).\Delta_{t,e,b} \quad (17)$$

$$SOE_{0,b}^{BS} = 0 \quad (18)$$

$$SOE_{t,b}^{BS} = SOE_{t-1,b}^{BS} - P_{t-1,b}^{BS,A} + SOE_{t,b}^{arr} \quad (19)$$

The inequality $\mathrm{SOE}_{(0,b)}^{BS}$ (20) stabilizes the initial state of the system, ensuring a consistent progression of the time series. Moreover, this requirement prevents the SOE variable from ever taking negative values, thereby preserving the physical validity of the model.

$$SOE_{0,b}^{BS} \geq 0 \quad (20)$$

To enable EV to supply power to BS, each vehicle must possess a sufficient amount of battery energy to reach the corresponding BS. Accordingly, for every EV $e \in E$ and every BS $b \in B$, an accessibility binary variable $\mathrm{REACH}_{e,b}$ (21) is introduced. This variable is determined by comparing the initial SOE of the EV with the travel energy required to reach BS b. A value of $\mathrm{REACH}_{e,b} = 1$ indicates that EV has adequate energy to reach the BS, whereas $\mathrm{REACH}_{e,b} = 0$ signifies that it does not.

$$\mathrm{REACH}_{e,b} = \begin{cases} 1, & if \;\; SOE_{e}^{\mathrm{init}} \geq E_{e,b}^{\mathrm{travel}} \\ 0, & otherwise \end{cases} \quad (21)$$

Based on these definitions, an EV can only be assigned to BSs that are energetically reachable, i.e., BSs for which the required travel energy does not exceed the vehicle's initial energy. Accordingly, the assignment variables $B_{(e,b)}^{(EV,L)}$ are restricted by this accessibility mask, which is formally expressed in (22).

$$B_{e,b}^{EV,L} \leq \mathrm{REACH}_{e,b} \quad (22)$$

If $\mathrm{REACH}_{e,b} = 0$, the assignment of EV e to BS b becomes mathematically infeasible; consequently, any physically unreachable assignment combinations are automatically excluded from the model. For each BS, the power consumed when the BS is active $P_{t,b}^{(BS,A)}$ (23), is expressed directly in terms of its nominal power capacity. This relationship is defined by the following equality:

$$P_{t,b}^{BS,A} = P_{b}^{c}.U_{t,b} \quad (23)$$

This equality expresses $P_{t,b}^{(BS,A)}$ as the power consumption of BS b at time t. The term P_b^c denotes the nominal power capacity of the BS, while $U_{t,b}$ (24) is a binary decision variable indicating whether the BS is active at that specific time step. When $U_{t,b} = 1$, the BS is operational and draws its nominal power; when $U_{t,b} = 0$, the BS is inactive and its power consumption becomes zero.

$$U_{t,b} \in \{0,1\} \quad (24)$$

The SOE of BS b at time t, expressed as $SOE_{t,b}^{BS}$(25), represents the total amount of energy stored at that BS. This quantity is constrained to remain non-negative at all times.

$$SOE_{t,b}^{BS} \geq 0 \quad (25)$$

A BS can be activated only if its SOE exceeds a predefined minimum operational threshold. This operational condition (26) is formulated as follows.

$$SOE_{t,b}^{BS} \geq SOE_{e}^{min}.U_{t,b} \quad (26)$$

When $U_{t,b} = 1$, BS b can be activated at time t; when, $U_{t,b} = 0$ BS b cannot be activated at time t. At the beginning of the post-disaster (i.e., t=0), all BS are assumed to be inactive (27). This assumption implies that no energy supply or EV deployment is available at the moment the disaster occurs. Consequently, it removes any ambiguity regarding the initial SOE of the BS and the timing of the first activation.

$$U_{0,b} = 0 \quad (27)$$

At each time step, the number of BSs that can be activated is physically limited by the number of available EV, since activating any BS requires at least one energy source. This constraint (28) is formulated as follows.

$$\sum_{b=0}^{TBSN-1} U_{t,b} \leq TEVN \quad (28)$$

With this approach, an upper bound is imposed on multiple BSs are activated that can be simultaneously active at any given time step. This constraint enhances the consistency of the model with real-world operational conditions and prevents physically infeasible scenarios involving unlimited BS activations. On the other hand, for a BS to become active, there must be at least one EV at its location. As mentioned earlier, activation is not possible in any location where there is no EV. This relationship is expressed as follows.

$$U_{t,b} \leq \sum_{e=0}^{TEVN-1} B_{e,b}^{EV,L} \quad (29)$$

As previously stated, the binary decision variable $B_{e,b}^{EV,L}$ indicates whether EV e is located at BS b. If no EV is assigned to BS b, the right-hand side of the constraint becomes zero, implying $U_{t,b} = 0$. A BS can be activated only if exactly one EV is located at that position and sufficient SOE is available.

Conversely, there is no activation at any BS where no EV is present, ensuring that $U_{t,b} \leq 1$.

The activation of a BS b is not solely contingent upon an EV e being assigned to that BS but also requires that the EV physically arrives there within a specific time step t. For this reason, BS activation is formulated with explicit consideration of EV arrival times. As previously introduced, the arrival indicator $\Delta_{t,e,b}$ (8) captures this temporal condition. Considering these conditions, an arrival matrix $A^{\text{arr}}_{t,e,b}$ (30) is defined to indicate whether an EV remains present at a BS b during all time steps following its arrival. This matrix captures the temporal persistence of an EV at BS after it reaches the location.

$$A^{\text{arr}}_{t,e,b} = 1\left(\sum_{\tau=1}^{t} \Delta_{[\tau,e,b]} > 0\right) \tag{30}$$

This expression indicates whether the EV has arrived at the BS at some time $\tau \leq t$. Accordingly, the indicator $A^{\text{arr}}_{t,e,b}$ takes the value 1 for all time steps following the arrival of EV e at BS b. The activation of a BS is formalized through the product of the assignment variable and the arrival matrix. This relationship (31) is expressed formally by the following equality.

$$U_{t,b} \leq \sum_{e \in E} B^{EV,L}_{e,b} \cdot A^{arr}_{t,e,b} \tag{31}$$

The capability of a BS to be activated precisely at the moment of an EV's arrival is represented by the variable $U^{\text{can}}_{t,b}$ (32). This binary decision variable, $U^{\text{can}}_{t,b} \in \{0,1\}$, takes the value 1 only at the exact time step when the EV reaches BS b, and remains 0 at all other times.

$$U^{can}_{t,b} = \sum_{e=0}^{TEVN-1} B^{EV,L}_{e,b} \cdot \Delta_{t,e,b} \tag{32}$$

The variable $U^{\text{can}}_{t,b}$ functions as a binary triggering mechanism within the decision structure of the model. When an EV arrives at its corresponding BS, this variable enables the initiation of activation at time t. If an EV is both assigned to that BS and reaches it at the exact arrival time, then $U^{\text{can}}_{t,b} = 1$, thereby allowing the BS to be activated. In summary, $U^{\text{can}}_{t,b}$ is an internal model variable that triggers a specific decision mechanism. In contrast, $\Delta_{t,e,b}$ is a pre-computed indicator determined by parameters such as travel distance, average speed, and departure time. With respect to the energy threshold, the arrival of an EV alone is not sufficient for activating a BS at the moment of arrival; the minimum required energy level must also be satisfied. This condition is formally imposed by constraint (33).

$$(SOE^{BS}_{t-1,\ b} + SOE^{arr}_{t,b}) \geq (SOE^{min}_{e}) \cdot U^{can}_{t,b} \tag{33}$$

When this energy threshold is satisfied, the activation of the BS becomes appropriate and is mandatorily triggered (34). However, if the required energy level is not available, the BS remains inactive even if $U^{\text{can}}_{t,b} = 1$; in such cases, the energy-threshold constraint prevents activation.

$$U_{t,b} \geq U^{can}_{t,b} \tag{34}$$

Base Station Deactivation Condition

The activation status of each BS at time is represented by the binary decision variable $U_{t,b} \in \{0,1\}$, as previously defined. A transition of a BS from the active state to the inactive state (i.e., $1 \rightarrow 0$) is classified as a *deactivation event*. To capture this event, a binary indicator $U^{off}_{t,b} \in \{0,1\}$(35) is utilized. The detection of a deactivation event is formally defined by the following linear inequality:

$$U^{off}_{t,b} \geq U_{t-1,b} - U_{t,b} \tag{35}$$

Considering this shutdown indicator, inequality (36) provides a consistent criterion for determining the physical conditions under which a BS can transition from an active state to a shutdown state. The left-hand side of the inequality,

$$SOE^{BS}_{t-1,b} + SOE^{arr}_{t,b}$$

Represents the total amount of energy effectively available at BS at the beginning of time step t. This total consists of the energy carried over from the previous minute, $SOE^{BS}_{t-1,b}$, and the net arrival energy $SOE^{arr}_{t\,b}$, which is transferred only if an EV reaches the BS precisely at minute t. The arrival energy is zero at all other time steps. The right-hand side of the inequality,

$$SOE^{min}_{e} + P^{c}_{b}$$

Defines the highest permissible energy level at which a shutdown event can be considered physically feasible. This threshold ensures that the BS cannot be switched off as long as it possesses sufficient energy to meet its mandatory safety reserve SOE^{min}_{e} and its nominal one-minute power demand P^{c}_{b}. Therefore, a shutdown is physically meaningful only when

$$SOE^{BS}_{t-1,b} + SOE^{arr}_{t,b} \leq SOE^{min}_{e} + P^{c}_{b}$$

Is satisfied.

The Big-M term,

$$M^{off}_{b}(1 - U^{off}_{t,b})$$

Ensures that this threshold condition is enforced only when the model attempts to issue a shutdown decision. If $U^{off}_{t,b} = 1$ (i.e., a shutdown is being attempted), the Big-M term vanishes and the inequality becomes binding; in this case, if the total energy exceeds the threshold, constraint (36) would be violated, preventing the model from shutting down the BS. Conversely, if no shutdown is triggered ($U^{off}_{t,b} = 0$), the large value of M^{off}_{b} relaxes the constraint, avoiding any artificial restriction on the natural evolution of the energy stock and allowing the BS to continue operating normally. Bringing all components together, the shutdown condition is formally expressed as: $SOE^{BS}_{t-1,b} + SOE^{arr}_{t,b}$

$$\leq SOE_e^{min} + P_b^c + M_b^{off} (1 - U_{t,b}^{off}) \quad (36)$$

This formulation ensures that BS shutdowns occur only under physically meaningful energy conditions, thereby preserving both the operational realism and the temporal consistency of the model.

Coverage Cells and Total Population

In this section, to enable an accurate assessment of the total covered area and total covered population, the coverage areas of the BSs are considered not only in terms of their geographic locations but also with respect to their mutual overlap relationships. Accordingly, the model defines two fundamental concepts using the cell-based coverage map $S_{b,c}$.

Pattern coverage: refers to regions in which multiple BSs simultaneously cover the same cell.

Single coverage: refers to cells that are covered exclusively by a single BS.

This distinction eliminates potential double-counting issues, ensuring that the population contained within each cell is accounted for exactly once in all calculations. Definition of Cells and Population Density:

- Cell area: $A_{\text{cell}} = \text{PCA}$ [km²/cell]
- Cell population density: ρ_c[people/cell]

The coverage status of the BSs is represented by the binary matrix $S_{b,c} \in \{0,1\}$. This matrix identifies, for each cell, which BS provide coverage, thereby explicitly characterizing the active coverage relationships across the grid. Subsequently, these two data sets are aggregated within a linear framework by linking them to the time dependent activation status of the BS. The notation used throughout this formulation is as follows: $b \in \{1, \dots, B\}$ denotes the set of BSs; $c \in \{1, \dots, C\}$ denotes the grid cells; $p \in \{1, \dots, P\}$ represents the coverage patterns; and $t \in \{1, \dots, T\}$ corresponds to the time steps.

Pattern Coverage

In this study, a pattern is defined as a subset of cells that are simultaneously covered by multiple BS. Each pattern p is represented by a vector indicating which BS contribute to that pattern. The pattern–BS relationship is expressed by the binary parameter $PT_{p,b} \in \{0,1\}$, where $PT_{p\,b} = 1$ denotes that BS b is part of pattern p.

$$PT_{p,b} = \begin{cases} 1 \text{ if BS b is part of pattern p} \\ 0 \qquad\qquad otherwise \end{cases} \quad (37)$$

Coverage Cell and Pattern

The pattern to which a cell belongs is determined by the exact matching between its coverage vector and the corresponding pattern vector.

$$M_{p,c} = \begin{cases} 1, & PT_P = S_c \\ 0, & otherwise \end{cases} \quad (38)$$

In other words, a cell is regarded as belonging to a particular pattern if the set of BSs covering that cell coincides exactly with the BS set defined by that pattern.

Single Coverage

In order to obtain the cell-level coverage structure of the BSs in a detailed manner, the coverage degree deg(c)(39) associated with each cell is first defined. For this purpose, by using the binary coverage matrix $S_{b,c} \in \{0,1\}$ defined over the set B of BSs and the set of C cells (where $S_{b\,c} = 1$ if BS b covers cell c), the coverage degree of each cell is computed as

$$\deg(c) = \sum_{b \in B} S_{b,c}\,, \quad c \in C \quad (39)$$

The coverage degree deg (c) indicates how many different BSs cover cell c, and it plays a fundamental role in determining the single-coverage condition. Accordingly, in order to distinguish the cells that are covered by only one BS, a cell-based binary singularity indicator (40) is defined as

$$H_c = \begin{cases} 1\,, & \text{if } \deg(c) = 1, \\ 0\,, & \text{otherwise,} \end{cases} \quad c \in C \quad (40)$$

This indicator mathematically labels the cells under single coverage and enables the separation of multiple-overlap regions within the coverage matrix. To extend the single-coverage structure to the BS–cell dimension, the indicator H_c is multiplied by the coverage matrix, and a new matrix (41) is obtained as

$$G_{b,c} = S_{b,c}\, H_c, \qquad b \in B,\, c \in C \quad (41)$$

Thus, $G_{b,c} = 1$ occurs only under the following conditions: (i) cell is under single coverage $(H_c = 1)$, and (ii) the only BS covering this cell is b $(S_{b,c} = 1)$. Therefore, the matrix $G_{b,c}$ precisely identifies the single-coverage area specific to each BS by automatically separating multi-coverage areas and uncovered cells. Using this structure, the total number of cells in the single-coverage area of BS b is defined as

$$N_b^{sgl} = \sum_c G_{b,c} \quad (42)$$

and it is employed as a quantitative indicator of the single-coverage capacity.

Computation of Average Single-Coverage Population Density

For each BS, the number of cells exclusively covered by that BS was defined earlier. Building on this definition, the total population residing within these single-coverage cells is denoted by R_b^s (Equation 43).

$$R_b^s = \sum_c G_{b,c} \cdot \rho_c \quad (43)$$

By taking the ratio of these quantities, the average population density under single coverage for each BS is obtained as $\bar{\rho}_b^s$ (44).

$$\bar{\rho}_b^s = \frac{R_b^s}{\max\left(N_b^{sgl}\right)} \tag{44}$$

Computation of Average Pattern-Based Population Density

In this expression, n_p (45) denotes the total number of cells covered by pattern p. Each pattern p represents a structural coverage configuration characterized by its own distinct set of BS.

$$n_p = \sum_c M_{p,c} \tag{45}$$

R_p (46) represents the total population contained within the cells covered by pattern p and is expressed as follows.

$$R_p = \sum_c M_{p,c}.\rho_c \tag{46}$$

In this context, R_p captures the aggregate population contained solely within the cells associated with pattern p. Patterns corresponding to densely populated regions naturally yield larger R_p values, whereas those representing rural or sparsely populated areas exhibit comparatively lower population totals. Consequently, through these two expressions, the average population density for pattern p, denoted by $\bar{p}_p$ (47), is obtained.

$$\bar{p}_p = \frac{R_p}{\max\left(n_p\right)} \tag{47}$$

Population and Cell Count Coefficients

α_p: expresses the number of grid cells associated with coverage pattern p, that is, the cells jointly covered by the same combination of BS. Likewise, α_b expresses the number of grid cells that are exclusively covered by BS b, with no overlap from any other BS. Using these parameter values, the total population within the single coverage area of BS b a fixed coefficient is computed as φ_b.

$$\varphi_b = \alpha_b.\bar{\rho}_b^s \tag{48}$$

The total number of people contained within the region corresponding to pattern p, which represents the overlap area, is computed as a fixed coefficient and is expressed as φ_b (49).

$$\varphi_p = \alpha_p.\bar{p}_p \tag{49}$$

Pattern Activation Constraint

For a pattern p to be activated ($Z_{p,t} = 1$), at least one of the BSs constituting that pattern must be active, and this requirement is expressed by inequality (50). If pattern p is not active ($Z_{p,t} = 0$), none of the BSs associated with that pattern is allowed to operate, and this condition is captured by inequality (51).

$U_{t,b} \in \{0,1\}$ BSs activation decision variable

$Z_{p,t} \in \{0,1\}$ Pattern activation variable, whether pattern p is active at time t is determined by its corresponding activation variable.

$$\sum_{b\in B} U_{t,b} \geq Z_{p,t}, \tag{50}$$

$$U_{t,b} \leq Z_{p,t} \tag{51}$$

Total Population Served

At time step t, the total population served is defined as the weighted aggregation of all active coverage patterns and active single-coverage BS regions, where φ_p denotes the population weight of pattern p and φ_b represents the mean population coefficient associated with the single-coverage area of BS b. This relationship is expressed as

$$POP_t = \left(\sum_{p\in P} \varphi_p \,.Z_{p,t} + \sum_{b\in B} \varphi_b.U_{t,b}\right)[person] \tag{52}$$

Objective Function

The objective is to maximize the total number of people served within the communication coverage area throughout the disaster period. This is formulated as follows in (53).

$$\max \sum_{t=1}^{AS} POP_t \tag{53}$$

This objective function implicitly governs the allocation of energy-supplying EV to BS by steering the optimization process toward configurations that yield the greatest communication reach. In effect, it mathematically determines which subsets of BS should be activated so as to maximize the population maintained under operational coverage throughout the disaster period.

RESULTS

The case study focuses on the district of Antakya, located in the Eastern Mediterranean region of Türkiye and one of the areas most severely affected by the Kahramanmaraş earthquakes of 6 February 2023. The test system consists of 20 BSs serving all mobile network operators in Antakya and 10 EVs that can be deployed as mobile power sources. The initial SOE levels of the EV fleet are provided in Table 1. For operational safety, each EV is assigned a minimum SOE threshold of $SOE_e^{min} = 1000 * 60\,[Watt.min]$ (17) (1 kWh), which must be preserved in the battery at all times and cannot be used for powering BSs. For mobility modeling, a constant travel-energy consumption rate of $\gamma = 9000$

Table 1. The initial (SOE) of the EVs.

EVs	Initial SOE (kWh)
1	71
2	66
3	61
4	56
5	51
6	46
7	41
8	36
9	31
10	26

W·min per kilometer is assumed for all EV, reflecting an average traction demand during displacement. Additionally, the average travel speed of the EVs is modeled as uniform and set to $V_{ev} = 50/60$ km per minute, providing a consistent basis for computing travel times across the network. During the earthquake, 64 of the 67 rooftop BSs in Antakya were destroyed or severely damaged, whereas 32 of the 34 tower-type BSs remained operational [9]. Consistent with these findings, a tower-based configuration representative of urban/suburban deployments has been adopted as the reference model in this study. In the population model used in this case study, cells located outside all macro-circles but within the coverage area of at least one BS are assigned a density of $P_c = 20$ people per cell, while cells lying outside both macro-circles and BS coverage areas are assigned $P_c = 5$ people per cell.

The proposed MILP model was developed in Python and solved using the Gurobi Optimizer (version 11.0.3). All simulations were performed on a computer with an Intel i5-7200U processor and 12 GB of memory. The total solution time for the Antakya case study was approximately 31 minutes.

The power requirements of BS vary on the order of several kilowatts, depending on factors such as radio configuration, transmission power, and site-specific auxiliary loads (e.g., cooling). Capacity-oriented small-cell deployments in higher frequency bands (e.g., 1800–2600 MHz) typically consume up to approximately 1 kW[10] [11], whereas macro sites operating in sub-GHz bands (e.g., 700/800/900 MHz) and providing wide-area coverage may require 5 kW or more when cooling and ancillary systems are included [4][12][13]. Cooling alone often accounts for 25–30% of total site energy consumption[14][15]. For this reason, the study incorporates different BS types. The BS-specific power demands and coverage radii used in the case study are reported in Table 2.

In this model, the EVs begin supplying power to the BSs starting from minute 2. By minute 21, all EVs have reached

Table 2. Coverage areas and power consumption of BSs.

BS index	BSs coverage area (km²)	BSs power (Watt)
1	3.7	4000
2	4.1	5000
3	4.5	6000
4	5	4500
5	5.7	5500
6	6.6	6500
7	6.9	4200
8	4.1	5200
9	4.5	6200
10	5.1	4800
11	5.7	5800
12	6.4	6800
13	6.9	4100
14	4.1	5100
15	4.7	6100
16	5.1	4300
17	5.8	5300
18	6.4	6300
19	6.9	4900
20	4.1	5900

their assigned BSs and have energized them using their arrival SOE $SOE_{t,b}^{arr}$. At minute 21, the total number of people able to maintain communication reaches its maximum value of 17,597, as demonstrated in Figure 3. This result is reported in Table 3.

The matching between the EV and the BS is provided in Table 3. Based on these assignments, the energy consumed by each EV while traveling to its designated BS is computed,

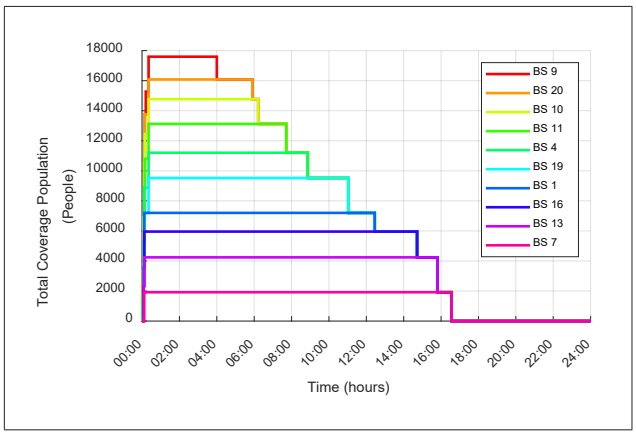

Figure 3. Population covered by bss post-disaster (people).

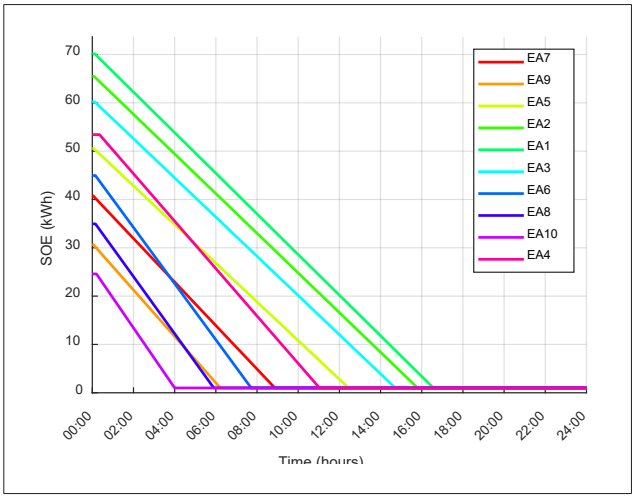

Figure 4. EV SOE at the time of post-disaster BS energization.

Table 3. The energization of BSs by EVs as a function of activation time, and the total number of people able to communicate.

Activation time [Min]	EVs	BSs	Total coverage population [People]
t=2	7	4	1.544
t=3	9	10	3.372
t=4	5	1	4.460
t=5	2	13	6.666
t=7	1	7	10.575
t=7	3	16	10.575
t=9	6	11	14.038
t=9	8	20	14.038
t=12	10	9	15.673
t=21	4	19	17.597

Table 4. EV arrival SOE at BSs and EV–BS distances.

Activation Time [Min]	EVs	BSs	Distance between EVs and BSs [km]	EVs arrival SOE [kWh]
t=2	7	4	1.4	40.78
t=3	9	10	2.4	30.65
t=4	5	1	2.9	50.56
t=5	2	13	3.4	65.49
t=7	1	7	5.6	70.16
t=7	3	16	5.2	60.22
t=9	6	11	7	44.95
t=9	8	20	7	34.96
t=12	10	9	9.3	24.6
t=21	4	19	17.2	53.42

and the resulting arrival SOE $SOE_{t,b}^{arr}$ is determined. These arrival energy values are reported in Table 4. In addition, the minute-by-minute energy consumption of each BS starting from the moment the EV reaches and energizes the site is illustrated in Figure 4.

CONCLUSION

This study develops a MILP framework for dispatching a fleet of EVs to energize BSs during disaster-induced outages, with the objective of maximizing population-based temporal connectivity under energy constraints. In the Antakya case study (20 BS, 10 EV), the optimization yields an extended early-stage service window, maintaining communication access for 17,597 individuals over a period of 228 minutes. As the EVs gradually deplete their energy reserves, the total covered population correspondingly declines, and service ceases at 16:34 local time. These findings demonstrate a viable approach to enable post-disaster communication access without the need for additional fixed generation resources. Moreover, integrating multi-objective planning and hybrid power resources (e.g., fuel-cell EVs, mobile power generators, or battery trucks) could further enhance operational effectiveness. Overall, the model offers a streamlined tool and field-deployable mission plans for emergency managers.

AUTHORSHIP CONTRIBUTIONS

Authors equally contributed to this work.

DATA AVAILABILITY STATEMENT

The authors confirm that the data that support the findings of this study are available within the article. Raw data that support the finding of this study are available from the corresponding author, upon reasonable request.

CONFLICT OF INTEREST

The authors declared no potential conflicts of interest with respect to the research, authorship, and/or publication of this article.

ETHICS

There are no ethical issues with the publication of this manuscript.

REFERENCES

[1] Unal S, Dagteke SE. Enhancement of fuel cell based energy sustainability for cell on wheels mobile base

stations used in disaster areas. Int J Hydrogen Energy, 2024;75:567–577. [CrossRef]

[2] Kimblad E. Assessing Critical Infrastructure Resilience: a case study of the 2023 Kahramanmaraş earthquakes Holistic Assessment of Critical Infrastructure Resilience during Disasters (HACIRD)-A case study of the 2023 Kahramanmaraş earthquakes. Available at: http://www.risk.lth.se Accessed on Jan 05, 2026

[3] Silva CMMRS, Premadasa PND, Chandima DP, Karunadasa JP, Wheeler P. Optimum sizing and configuration of electrical system for telecommunication base stations with grid power, Li-ion battery bank, diesel generator and solar PV. J Energy Storage 2025;123:116704. [CrossRef]

[4] Rahman MRU, Niknejad P, Barzegaran MR. Resilient Hybrid Energy System (RHES) for Powering Cellular Base Transceiver Station during Natural Disasters. 2021 IEEE Power and Energy Conference at Illinois, *PECI 2021*, Institute of Electrical and Electronics Engineers Inc., 2021. [CrossRef]

[5] Okundamiya MS, Emagbetere JO, Ogujor EA. Assessment of renewable energy technology and a case of sustainable energy in mobile telecommunication sector. Sci World J 2014;2014:947281. [CrossRef]

[6] Cabrera-Tobar A, Grimaccia F, Leva S. Energy resilience in telecommunication networks: A comprehensive review of strategies and challenges. Energies (Basel) 2023;16:6633. [CrossRef]

[7] Curran Associates. 2017 International Conference on Industrial Engineering, Applications and Manufacturing (ICIEAM) : proceedings : South Ural State University (national research university), Chelyabinsk, Russia, May 16-19, 2017. IEEE, 2017.

[8] Ahmed F, Naeem M, Ejaz W, Iqbal M, Anpalagan A, Kim HS. Renewable energy assisted traffic aware cellular base station energy cooperation. Energies (Basel) 2018;11:99. [CrossRef]

[9] Türkiye Bilişim Derneği. Türkiye Bilişim Derneği Türkiye'nin Deprem Gerçeği: Bilişim Çözümleri Deprem ve Bilişim Çalıştayı Raporu Çalıştay Tarihi Raporu. Türkiye Bilişim Derneği. Available at: https://www.tbd.org.tr/en/tbd-deprem-ve-bilisim-calistayi-raporu/ Accessed on Jan 05, 2026.

[10] Deevela NR, Kandpal TC, Singh B. A review of renewable energy based power supply options for telecom towers. Environ Dev Sustain 2024;26:2897–2964. [CrossRef]

[11] Gandotra P, Jha RK, Jain S. Green communication in next generation cellular networks: A survey. IEEE Access 2017;5:11727–11758. [CrossRef]

[12] Lorincz J, Garma T, Petrovic G. Measurements and modelling of base station power consumption under real traffic loads. Sensors 2012;12:4281–4310. [CrossRef]

[13] Kusakana K, Vermaak HJ. Hybrid renewable power systems for mobile telephony base stations in developing countries. Renew Energy 2013;51:419–425. [CrossRef]

[14] Yeshalem MT, Khan B. Design of an off-grid hybrid PV/wind power system for remote mobile base station: A case study. AIMS Energy 2017;5:96–112. [CrossRef]

[15] Rahman M. Overview of energy saving aspects in 2G and 3G Mobile Communication Networks (Master thesis). Swedish: University of Gävle; 2009.